Journal of Movement & Neuromuscular Science
Published by Noventra Scientific Publishing
Website: movementneuromuscular.org • Email: editorial@movementneuromuscular.org

ORIGINAL RESEARCH OPEN ACCESS

Myoelectric Manifestations of Fatigue in Sport: Evidence from Repeated Maximal Shooting in Professional Water Polo

Filippo Cotellessa[1], Halil İbrahim Ceylan[2], Nicola Luigi Bragazzi[3], Luca Puce[1,*]

Filippo Cotellessa: ORCID: 0009-0007-8518-365X
Halil İbrahim Ceylan: ORCID: 0000-0003-1133-5511
Nicola Luigi Bragazzi: ORCID: 0000-0001-8409-868X
Luca Puce: ORCID: 0000-0003-0825-2707

[1] Department of Neuroscience, Rehabilitation, Ophthalmology, Genetics, Maternal and Child Health, University of Genoa, Italy

[2] Physical Education and Sports Teaching Department, Faculty of Sports Sciences, Ataturk University, Erzurum 25240, Türkiye

[3] Department of Mathematics and Statistics, Laboratory for Industrial and Applied Mathematics (LIAM), York University, Toronto, Ontario (ON), Canada

Corresponding author: Luca Puce • luca.puce@medicina.unige.it

J Mov Neuromuscul Sci. 2026;1(1)

Received: 2 March 2026 | **Revised:** 28 July 2026 | **Accepted:** 10 August 2026 | **Published:** 2 September 2026

Abstract

Background: Repeated maximal sport actions may induce localized myoelectric alterations before external performance deteriorates. This study examined whether repeated maximal shooting in professional water polo produces fatigue-compatible myoelectric changes despite preservation of ball velocity.

Methods: Fourteen male professional players performed up to 20 consecutive maximal-effort 5-m penalty shots. Surface electromyography was recorded from 14 throwing-side and trunk muscles and synchronized with multi-view video and stereo-derived ball velocity. Median frequency within a standardized 200-ms late-cocking window was the primary spectral outcome. Phase-specific RMS amplitude, activation-weighted temporal centroid, movement-phase duration, and multimuscle activation-pattern reorganization were also evaluated. Muscle-specific spectral analyses were adjusted for within-athlete ball velocity and concurrent RMS amplitude, with false-discovery-rate correction for multiple comparisons.

Results: The dataset comprised 222 valid EMG shots, including 219 with matched ball velocity. Ball velocity was preserved across the shooting sequence (first five: 79.47 $km \cdot h^{-1}$; last five: 82.00 $km \cdot h^{-1}$; mean difference +2.53 $km \cdot h^{-1}$; p=0.055). Median frequency decreased significantly only in teres major (−14.62 Hz; 95% CI −22.71 to −5.89; q=0.0042) and the clavicular portion of pectoralis major (−10.08 Hz; 95% CI −17.18 to −4.93; q=0.0028). These effects remained directionally robust across alternative spectral specifications and leave-one-athlete-out analyses. Changes in activation amplitude and timing were heterogeneous, and neither complete-montage nor localized measures of EMG reorganization were associated with ball velocity.

Conclusions: Repeated maximal shooting in professional water polo produced selective fatigue-compatible myoelectric changes despite preserved ball velocity. External performance may therefore remain stable while localized myoelectric alterations are already detectable, highlighting the value of combining muscle-specific physiological measures with performance outcomes during repeated explosive sport actions.

Keywords: surface electromyography; muscle fatigue; median frequency; water polo; throwing; ball velocity; overhead throwing; neuromuscular fatigue

1. Introduction

Muscular fatigue is a fundamental constraint on sports performance, particularly when high-intensity actions must be repeated with limited recovery. Rather than representing a single physiological process, fatigue arises from interacting peripheral and central mechanisms that modify the capacity of the neuromuscular system to meet task demands [1–3]. Importantly, these internal changes do not necessarily produce an immediate deterioration in observable performance. Skilled athletes may temporarily preserve force, velocity, or technical outcome despite fatigue-related physiological alterations, making external performance alone an incomplete indicator of the underlying neuromuscular state [3]. This distinction is particularly relevant in elite sport, where training status and adaptive motor strategies may delay the point at which fatigue becomes evident as performance loss.

Surface electromyography (sEMG) provides a non-invasive means of examining muscle-specific myoelectric manifestations associated with fatigue during exercise [4–6]. Amplitude- and frequency-domain features provide complementary, but not interchangeable, information. Surface-EMG amplitude is influenced by motor-unit recruitment and discharge behavior, as well as by action-potential cancellation, electrode position, muscle geometry, muscle length, and contraction velocity [6, 7]. Spectral analysis provides a complementary perspective. During fatiguing contractions, the EMG power spectrum commonly shifts toward lower frequencies, reflected by reductions in measures such as median or mean frequency and associated with changes in muscle-fiber conduction and motor-unit behavior [4, 5]. Interpretation is more challenging during dynamic sporting movements because rapid changes in muscle length, contraction velocity, force, and electrode–muscle geometry introduce substantial non-stationarity into the signal [7]. Time–frequency approaches are therefore particularly useful for examining spectral behavior within short, movement-specific windows [8], and spectral sEMG parameters have shown utility for detecting fatigue-related myoelectric changes during dynamic swimming exercise [9]. Accordingly, spectral changes observed during dynamic exercise are most appropriately interpreted as fatigue-compatible myoelectric manifestations rather than as direct quantitative measures of biological fatigue.

These interpretative challenges are particularly relevant during repeated explosive sport actions, in which brief maximal efforts are performed in succession and the external task outcome may remain stable despite evolving neuromuscular demands. This issue becomes especially important when performance depends on the integrated contribution of multiple body segments rather than on the output of a single muscle or joint. Within this context, repeated maximal shooting in water polo provides a useful sport-specific model for examining the potential dissociation between localized myoelectric changes and external performance. The water polo shot is a high-velocity action performed without a stable support base and requires coordinated contributions from body elevation, trunk motion, and upper-limb acceleration [10, 11]. Ball velocity therefore represents the integrated result of a complex whole-body action. Importantly, increasing fatigue can impair technical performance without necessarily producing a proportional decline in shooting velocity [12].

Previous electromyographic studies have characterized upper-extremity muscle activation during water polo shooting and demonstrated differences in activation magnitude, timing, and proximal-to-distal organization between experienced and inexperienced performers [13, 14]. Kinematic studies have additionally documented substantial intraindividual variability in the organization of the 5-m shot despite comparatively stable performance outcomes [15]. However, these studies have primarily characterized individual shooting actions or between-group differences. It remains unclear how muscle-specific myoelectric manifestations evolve during a sequence of repeated maximal shots, whether fatigue-compatible spectral changes emerge uniformly or selectively across the throwing musculature, and whether such changes occur despite preservation of ball velocity. It is likewise unknown whether repeated shooting is accompanied by systematic changes in activation amplitude or timing that could contribute to maintenance of the external performance outcome.

Against this background, the present study examined muscle-specific myoelectric changes during repeated maximal shooting in professional water polo players while ball velocity was monitored simultaneously. Surface EMG was recorded from a 14-muscle throwing-side and trunk montage across

preparation, cocking, acceleration, and deceleration, with fatigue-compatible spectral changes evaluated within a standardized late-cocking window. The primary aim was to determine whether repeated maximal shooting produced selective or generalized spectral manifestations compatible with fatigue and whether these changes occurred despite preserved ball velocity. Secondary analyses examined phase-specific activation amplitude and timing and explored whether myoelectric change or activation-pattern reorganization was associated with ball velocity. We hypothesized that fatigue-compatible spectral changes would be muscle-specific rather than uniform and could emerge despite preservation of external performance.

2. Materials and Methods

2.1. Study design, participants, and ethics

This single-session repeated-measures study included 14 male professional field players from one team competing in the Italian A1 league. All athletes were actively training and competing at the time of testing. Exclusion criteria were acute upper-extremity or trunk injury, previous surgery to the throwing shoulder, neurological disorders affecting upper-extremity motor function, or intolerance to surface-electrode placement. Players with non-limiting shoulder symptoms were not excluded, provided that they were able to perform maximal-effort shooting.

The study was conducted in accordance with the Declaration of Helsinki and was approved by the Comitato Etico per la Ricerca di Ateneo (CERA; approval no. 2024.55, 14 June 2024). All participants provided written informed consent before testing.

2.2. Shooting protocol, video acquisition, and ball velocity

After electrode placement, players completed a warm-up consisting of freestyle swimming and practice shots. Each player then performed up to 20 consecutive maximal-effort penalty shots from the official 5-m line. Approximately 5 s separated consecutive attempts, during which a poolside assistant returned the ball to the player. A shot was excluded from a specific analysis when the ball bounced before reaching the goal or when the data required for that analysis were incomplete. The final EMG dataset comprised 10–19 valid shots per athlete. The chronological order of retained valid shots was preserved throughout the analyses; when an observation was unavailable for a specific downstream analysis, subsequent valid shots retained their original within-series position and were not renumbered.

Three GoPro HERO8 cameras (GoPro, San Mateo, CA, USA) recorded the shooting action at 120 frames·s^{-1} and were positioned to provide frontal/goal-line, lateral, and approximately 45° diagonal views. Before data acquisition, the frontal and lateral cameras were stereo-calibrated using a checkerboard calibration target. The synchronized calibrated frontal and lateral recordings were used to reconstruct the ball trajectory, whereas the diagonal camera provided an additional view for movement-event identification and was not used for stereo reconstruction.

Ball release was operationally defined as the first video frame in which no visible contact between the throwing hand and the ball remained. Ball velocity was derived from the stereo-reconstructed trajectory and calculated as the mean of the ball-speed values obtained over the first four post-release frames, beginning with the first frame showing complete loss of hand–ball contact. Velocity was expressed in km·h^{-1} and assigned to the corresponding athlete and shot.

Video and EMG recordings were synchronized using a common physical synchronization event. The cameras recorded the EMG sensor positioned over the biceps while an operator delivered a brief tap directly to the sensor. The tap was visually identifiable in the video recordings and simultaneously generated a sharp transient artifact in the EMG trace, providing a common temporal reference for alignment of the video and EMG signals.

Movement events were identified by an operator through frame-by-frame visual inspection of the synchronized recordings. Five events were marked: (1) start of preparation, (2) start of cocking, (3) start of acceleration, (4) ball release/start of deceleration, and (5) end of deceleration (Figure 1). These events delimited four movement phases: preparation, cocking, acceleration, and deceleration. With the

exception of ball release, which was operationally defined as described above, the remaining events were identified visually from the movement sequence rather than from predetermined kinematic thresholds.

2.3. Surface EMG acquisition

Surface electromyography was recorded at 2,000 Hz using a MiniX Waterproof wireless system (Cometa, Italy) and disposable bipolar Kendall Ag/AgCl surface electrodes. Before electrode placement, the skin was shaved when necessary, lightly abraded, and cleaned with alcohol. Electrodes were positioned over the muscle belly and aligned with the presumed direction of the underlying muscle fibers, following SENIAM recommendations where applicable and established recommendations for surface-EMG acquisition and reporting [16, 17].

Recordings were obtained from 14 muscles on the throwing side: flexor carpi radialis, biceps brachii, lateral triceps, anterior deltoid, middle deltoid, posterior deltoid, pectoralis major, clavicular portion, pectoralis major, sternocostal portion, teres major, infraspinatus, latissimus dorsi, middle trapezius, lower rectus abdominis, and thoracic erector spinae. All 14 channels were included in the phase-specific activation and spectral analyses.

For data acquisition and export, channel labels carried an "R_" prefix; this designation referred to the throwing side rather than necessarily to the anatomical right side. Accordingly, EMG was recorded from the left upper limb in the two left-handed throwers.

2.4. Raw-signal quality control and processing

All processing started from the raw, non-rectified sEMG signal. Samples were classified as invalid when data were missing or when absolute signal amplitude reached the acquisition-system saturation threshold of 3,290 digital units. A muscle–shot channel was excluded when more than 5% of the samples within the analyzed movement were invalid or when a constant-value segment persisted for at least 100 ms, indicating loss or corruption of the recorded signal. Isolated invalid samples within otherwise acceptable channels were replaced by linear interpolation. No channel-level data failing the predefined quality criteria were imputed.

Raw signals were filtered using a zero-phase frequency-domain passband from 20 to 450 Hz, with cosine transitions between 15–20 Hz and 450–500 Hz. Power-line interference was attenuated using a 50-Hz notch with cosine shoulders extending from 48.5 to 51.5 Hz. A centered 50-ms RMS envelope was subsequently calculated for amplitude-domain analyses. These procedures followed established principles for surface-EMG acquisition, preprocessing, and artifact control [6, 17].

For each athlete and muscle separately, the normalization reference was defined as the 95th percentile (P95) of the RMS envelope pooled across all valid trials. RMS amplitude was then expressed as a percentage of this athlete- and muscle-specific P95 reference. This task-based normalization provided a robust within-athlete, within-muscle reference while limiting the influence of isolated extreme peaks [18]. Because a separate P95 reference was calculated for each muscle and athlete, normalized amplitudes were interpreted within muscle and were not used as measures of absolute activation magnitude across different muscles or participants.

2.5. Fatigue-compatible spectral outcome

For each of the 14 recorded muscles, the primary spectral outcome was the median frequency of the sEMG signal estimated within a fixed 200-ms late-cocking window ending at the onset of acceleration. At the acquisition frequency of 2,000 Hz, each analysis window comprised 400 samples. All observed cocking phases were at least 204.5 ms in duration, allowing the same task segment to be examined across shots.

Median frequency was estimated using a continuous-wavelet time–frequency approach. Such approaches are particularly suitable for dynamic contractions in which conventional stationarity assumptions are difficult to satisfy [4, 5, 7–9]. Muscle-specific end-to-start changes across the shooting sequence were modeled while adjusting for within-athlete ball velocity and concurrent log-transformed RMS amplitude. Inclusion of concurrent RMS was intended to reduce the possibility that apparent spectral differences merely reflected concurrent differences in signal amplitude.

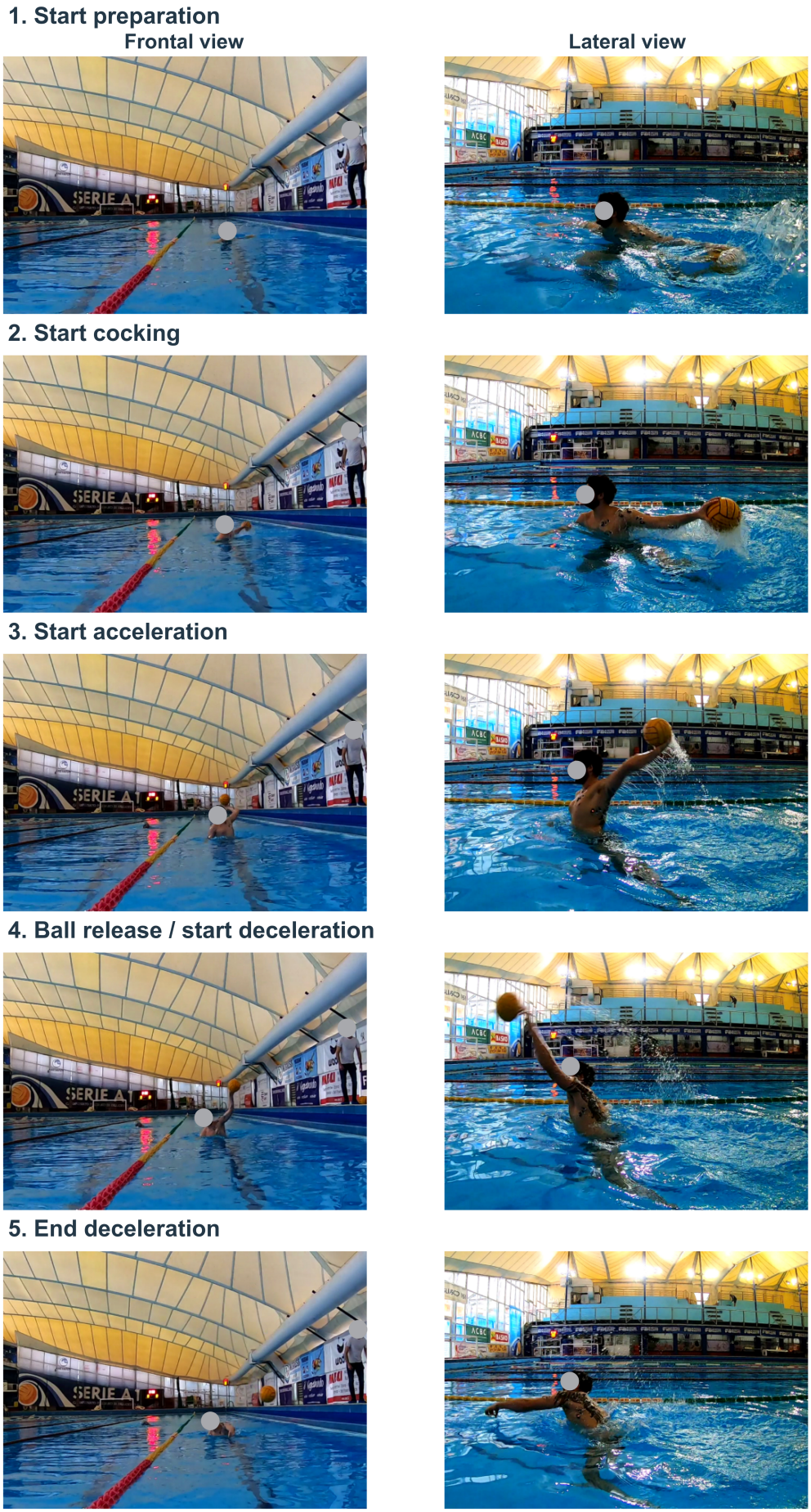


Figure 1: Shooting phases and movement events used to segment the maximal 5-m water polo shot.

For graphical presentation, shot-by-shot median-frequency changes were additionally expressed as percentage reduction relative to the athlete- and muscle-specific mean of the first five valid shots. These percentage values were used as normalized electrical indicators of fatigue-compatible change and were not interpreted as direct percentage measures of biological fatigue.

Robustness of the primary spectral findings was examined using alternative analytical specifications. These included matched lower-frequency cutoffs of 20, 30, and 40 Hz, fast Fourier transform estimation, restriction to active windows with RMS >10% of the athlete- and muscle-specific P95 reference, low-band trimming, first-three versus last-three contrasts, leave-one-athlete-out analyses, and chronological permutation.

2.6. Phase-specific activation, timing, and duration

Preparation, cocking, acceleration, and deceleration were independently time-normalized from 0% to 100% of their respective phase duration. For each muscle and shot, mean RMS-envelope amplitude and the activation-weighted temporal centroid were calculated separately within each phase.

The temporal centroid represented the relative position within the phase around which the RMS envelope was temporally concentrated, with lower values indicating an earlier and higher values a later distribution of activation. It therefore characterized within-phase activation timing rather than activation onset, peak timing, or motor-unit synchronization.

The absolute durations of the cocking and acceleration phases were additionally retained in milliseconds to evaluate whether changes in movement-phase duration accompanied repeated shooting or were associated with ball velocity.

2.7. Integrated activation–fatigue–performance analysis

For the phase-activation atlas, shot-level values were first averaged within athlete and then summarized across athletes so that participants contributing a greater number of valid shots did not receive disproportionate weight. Changes across the shooting series were additionally summarized by comparing each athlete's first five and last five valid shots for RMS amplitude and activation-weighted temporal centroid.

To quantify complete-pattern reorganization, each shot was represented by a 14-muscle × four-phase profile. Amplitude-pattern reorganization was calculated as the root-mean-square distance between the shot-specific log-transformed RMS-amplitude profile and the athlete's mean first-five profile. Temporal-pattern reorganization was calculated analogously using phase-normalized activation-weighted temporal centroids. Larger distance values therefore indicated greater deviation from the athlete's early-series activation pattern. Distances were calculated across available muscle–phase cells; at least 42 of the 56 possible cells were required, and missing cells were not imputed.

Two complementary spectral fatigue-burden indices were examined. The all-muscle burden summarized median-frequency reduction across all valid recorded muscles relative to the corresponding athlete- and muscle-specific first-five baseline. Because it incorporated the complete recorded montage without selecting muscles on the basis of their individual statistical results, this index was used as the non-selected complete-montage measure of spectral change.

A secondary localized burden was calculated using only the two muscles that met the FDR criterion in the preceding 14-muscle analysis—the clavicular portion of pectoralis major and teres major. Because these muscles were selected after inspection of the muscle-specific results, the localized burden was explicitly treated as a post-identification explanatory measure and not as independent confirmation of fatigue.

Integrated analyses required at least 10 valid spectral channels and sufficient phase data to meet the 42-of-56 cell criterion. Analyses involving the localized burden additionally required valid spectral data from both FDR-identified muscles. The final integrated dataset comprised 211 shots from all 14 athletes.

2.8. Statistical analysis

Athletes, rather than individual shots, defined the inferential clustering unit. Within each athlete, shot position was scaled from 0 for the first retained valid shot to 1 for the last retained valid shot. When an observation was unavailable for a specific downstream analysis, subsequent valid shots retained their original position within the retained shooting sequence and were not renumbered.

Repeated-measures regression models included athlete fixed effects to account for stable between-athlete differences and linear and quadratic terms for shot position to allow for non-linear changes across the shooting series. For each of the 14 muscles, median frequency was modeled as a function of shot position while adjusting for within-athlete ball velocity and concurrent log-transformed RMS amplitude. Muscle-specific end-to-start changes were obtained from the fitted sequence terms.

Statistical uncertainty for regression estimates was quantified using cluster-bootstrap resampling at the athlete level, thereby preserving dependence among repeated shots from the same player. Bootstrap distributions were used to derive 95% confidence intervals and two-sided p values for model coefficients.

For the comparison of ball velocity between the first five and last five valid shots, mean velocity was first calculated within athlete for each period. The athlete-level mean difference was reported together with an athlete-cluster bootstrap 95% confidence interval and an exact two-sided paired sign-flip p value. Because the confidence interval and p value were obtained from distinct inferential procedures, their numerical threshold decisions were not required to coincide exactly.

Multiplicity was controlled using the Benjamini–Hochberg false-discovery-rate (FDR) procedure [19]. FDR correction was applied across the 14 muscle-specific median-frequency tests and separately within each predefined family of activation–fatigue–performance models. An FDR-adjusted q value <0.05 was considered statistically significant.

Phase selectivity was summarized at the athlete level as the difference between each muscle's observed highest-amplitude phase and the mean amplitude of its remaining three phases. These contrasts were evaluated using paired sign-flip tests, with FDR correction across the 14 muscles. Athlete-level cluster-bootstrap 95% confidence intervals were additionally calculated for the phase-selectivity estimates. Because the highest-amplitude phase was identified from the same observed phase atlas, phase-selectivity inference was considered secondary and exploratory.

First-five versus last-five changes in phase-specific amplitude and temporal centroid were treated as descriptive athlete-level comparisons and summarized with bootstrap confidence intervals.

All analyses were performed in Python using reproducible analysis scripts. The processed datasets, variable definitions, and complete statistical outputs are provided in the accompanying analysis workbook.

3. Results

3.1. Participants and data completeness

The 14 professional players were 25.7 $\pm$ 6.1 years old, 184.1 $\pm$ 6.2 cm tall, and 89.2 $\pm$ 8.9 kg, with 14.6 $\pm$ 6.1 years of playing experience. Twelve were right-handed and two were left-handed throwers (Table 1).

The final dataset comprised 222 valid EMG shots, of which 219 had matched ball-velocity measurements. Across the 14-muscle montage, 2,957 of 3,108 possible late-cocking muscle–shot windows (95.1%) satisfied the predefined signal-quality criteria. The phase-activation atlas contained 11,876 of 12,432 possible muscle–phase–shot observations (95.5%), with 9–14 athletes contributing to individual muscle–phase cells. The integrated activation–fatigue–performance analyses included 211 shots from all 14 athletes (Supplementary Table S1).

Table 1: Participant characteristics.

Characteristic	Value
Players	14 male professional field players
Age, years	25.7 $\pm$ 6.1

Table 1: Participant characteristics.

Characteristic	Value
Height, cm	184.1 ± 6.2
Body mass, kg	89.2 ± 8.9
BMI, $kg \cdot m^{-2}$	26.3 ± 2.2
Playing experience, years	14.6 ± 6.1
Throwing-side dominance	12 right; 2 left

3.2. Ball velocity was preserved

Across the 219 velocity-matched shots, the descriptive shot-level mean ball velocity was 82.07 ± 11.89 $km \cdot h^{-1}$. At the athlete level, mean velocity was 79.47 $km \cdot h^{-1}$ during the first five valid shots and 82.00 $km \cdot h^{-1}$ during the last five, corresponding to a mean difference of +2.53 $km \cdot h^{-1}$ (bootstrap 95% CI 0.28 to 4.76; exact paired sign-flip p=0.055). Thus, repeated maximal shooting was not accompanied by a decline in ball velocity.

Across ordinal shot positions, velocity showed an initial rise followed by later attenuation rather than a progressive monotonic decrease (Figure 2).

3.3. Phase-specific activation across the 14-muscle montage

The four-phase atlas demonstrated marked within-muscle phase dependence across the recorded montage (Figure 3; Supplementary Figure S1). Eleven of the 14 muscles met the FDR criterion in the secondary phase-selectivity analysis.

Seven muscles showed their strongest relative activation during acceleration: flexor carpi radialis (+59.79 percentage points [pp], q=0.0012), pectoralis major, clavicular portion (+37.27 pp, q=0.0012), latissimus dorsi (+36.40 pp, q=0.0014), lateral triceps (+31.92 pp, q=0.0012), pectoralis major, sternocostal portion (+31.47 pp, q=0.0012), lower rectus abdominis (+29.99 pp, q=0.0012), and teres major (+20.91 pp, q=0.0248).

Preparation selectivity was observed for middle deltoid (+18.89 pp, q=0.0056) and middle trapezius (+14.74 pp, q=0.0248), whereas infraspinatus (+15.44 pp, q=0.0296) and thoracic erector spinae (+13.24 pp, q=0.0492) showed deceleration selectivity. No other amplitude phase-selectivity contrast met the FDR criterion (Supplementary Table S2).

Because RMS amplitude was normalized using a separate athlete- and muscle-specific P95 reference, the values displayed in Figure 3A describe within-muscle phase organization and should not be interpreted as absolute activation rankings between different muscles.

3.4. Fatigue-compatible spectral changes across the 14-muscle montage

The same 200-ms late-cocking window, covariate adjustment, and FDR-controlled analysis were applied to all 14 recorded muscles (Figure 4; Table 2; Supplementary Table S3). Only two muscles showed a reliable downward shift in median frequency across the shooting series. Teres major showed an adjusted end-to-start change of −14.62 Hz (95% CI −22.71 to −5.89; q=0.0042), whereas pectoralis major, clavicular portion showed a change of −10.08 Hz (95% CI −17.18 to −4.93; q=0.0028).

These were the only two muscles that met the FDR criterion across the complete 14-muscle analysis. Infraspinatus (−8.32 Hz), pectoralis major, sternocostal portion (−6.20 Hz), lower rectus abdominis (−4.78 Hz), and latissimus dorsi (−2.46 Hz) showed negative point estimates, but their confidence intervals included zero and none survived FDR correction (all q≥0.243). The remaining recorded muscles likewise showed no reliable downward median-frequency shift.

Notably, strong acceleration-phase activation selectivity did not necessarily coincide with fatigue-compatible spectral change. Flexor carpi radialis and lateral triceps showed two of the largest acceleration-selectivity contrasts, yet neither showed a significant reduction in median frequency. The shot-by-shot evolution of the two FDR-identified muscles is shown in Figure 5A.

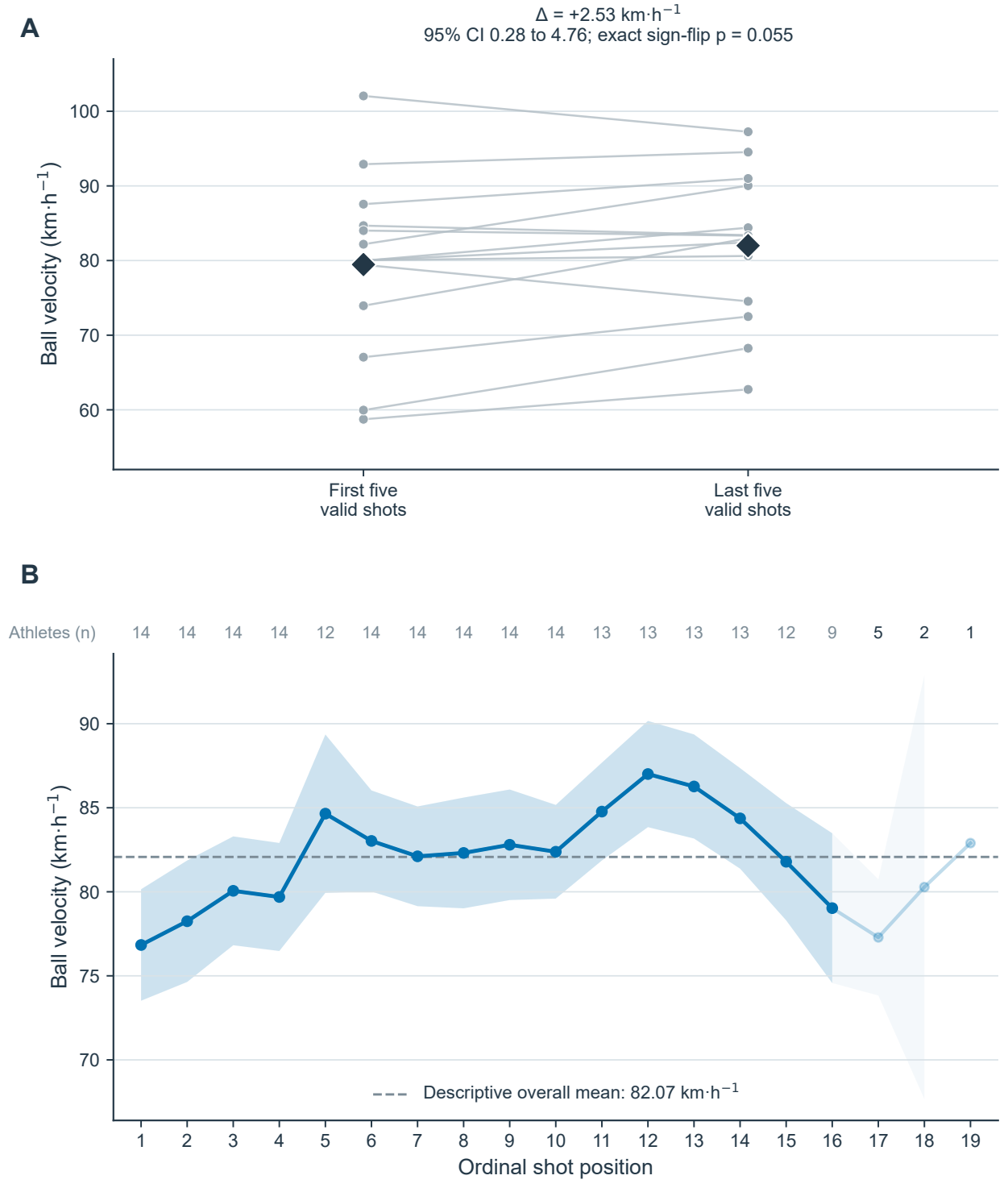


Figure 2: Ball velocity during repeated maximal shooting. (A) First versus last five valid shots. (B) Velocity across ordinal shot position; the number of contributing athletes is shown above each position.

Table 2: Complete 14-muscle fatigue-compatible spectral analysis.

Throwing-side muscle	Adjusted end-to-start change	95% CI	FDR q
Teres major	−14.62 Hz	−22.71 to −5.89	0.0042
Pectoralis major, clavicular portion	−10.08 Hz	−17.18 to −4.93	0.0028
Infraspinatus	−8.32 Hz	−23.51 to +7.55	0.624
Pectoralis major, sternocostal portion	−6.20 Hz	−12.26 to +0.04	0.243
Lower rectus abdominis	−4.78 Hz	−10.72 to +0.94	0.331
Latissimus dorsi	−2.46 Hz	−6.51 to +2.02	0.612
Biceps brachii	−1.30 Hz	−5.26 to +2.66	0.812
Lateral triceps	−1.05 Hz	−9.42 to +9.02	0.912
Posterior deltoid	−0.71 Hz	−5.72 to +2.54	0.899
Middle deltoid	−0.69 Hz	−7.05 to +3.22	0.912
Anterior deltoid	+0.05 Hz	−10.18 to +9.15	0.958
Flexor carpi radialis	+1.25 Hz	−5.96 to +9.02	0.899
Middle trapezius	+1.87 Hz	−3.59 to +8.44	0.812
Thoracic erector spinae	+4.81 Hz	−1.07 to +11.30	0.331

3.5. Integrated activation–fatigue–performance analysis

The non-selected all-muscle fatigue burden showed no reliable change across the shooting sequence (β=+0.42 standardized units, 95% CI −1.36 to +2.06; q=0.946). It was also not associated with amplitude-pattern distance (β=−0.13, 95% CI −0.36 to +0.12; q=0.946) or temporal-pattern distance (β=−0.01, 95% CI −0.22 to +0.16; q=0.946).

In the corresponding velocity model, ball velocity was not independently associated with the all-muscle fatigue burden (+0.26 $km \cdot h^{-1}$ per within-athlete SD, 95% CI −0.59 to +1.15; q=0.846), amplitude-pattern distance (+0.59 $km \cdot h^{-1}$, 95% CI −0.73 to +1.84; q=0.846), or temporal-pattern distance (+0.03 $km \cdot h^{-1}$, 95% CI −1.11 to +1.00; q=0.944). Neither the all-muscle fatigue × amplitude-pattern interaction (−0.32 $km \cdot h^{-1}$, 95% CI −1.58 to +0.66; q=0.846) nor the all-muscle fatigue × temporal-pattern interaction (+0.13 $km \cdot h^{-1}$, 95% CI −1.17 to +1.28; q=0.944) met the FDR criterion (Table 3; Supplementary Table S4).

The secondary localized burden, calculated from the clavicular portion of pectoralis major and teres major after these muscles had been identified in the preceding 14-muscle FDR analysis, increased across shot position (β=+1.78 standardized units, 95% CI +0.43 to +2.97; q=0.030). Because this index was defined post-identification, this sequence effect was not interpreted as independent confirmation of fatigue.

In the localized performance model, neither the localized fatigue burden (−0.01 $km \cdot h^{-1}$ per within-athlete SD, 95% CI −0.67 to +0.59; q=0.997), amplitude-pattern distance (+0.41 $km \cdot h^{-1}$, 95% CI −0.89 to +1.76; q=0.817), nor temporal-pattern distance (−0.004 $km \cdot h^{-1}$, 95% CI −0.92 to +0.89; q=0.997) was independently associated with ball velocity. Likewise, neither the localized fatigue × amplitude-pattern interaction (+0.50 $km \cdot h^{-1}$, 95% CI −0.94 to +1.64; q=0.761) nor the localized fatigue × temporal-pattern interaction (−1.07 $km \cdot h^{-1}$, 95% CI −2.46 to +0.28; q=0.277) met the FDR criterion (Figure 5C; Table 3).

Thus, neither the complete-montage nor the localized analysis identified a systematic EMG reorganization that statistically accounted for preserved ball velocity.

3.6. Phase-specific activation timing and phase duration

The activation-weighted temporal-centroid analysis showed distinct within-phase timing patterns across the recorded muscles (Figure 3C). During cocking, pectoralis major, clavicular portion (73.3% of phase), flexor carpi radialis (70.2%), pectoralis major, sternocostal portion (69.9%), and lower rectus abdominis (66.9%) showed activation distributions weighted toward the later portion of the phase.

During acceleration, middle deltoid (61.9%), posterior deltoid (60.4%), thoracic erector spinae (58.8%), middle trapezius (58.2%), and infraspinatus (57.7%) showed later temporal centroids, whereas both pectoralis major portions were weighted earlier within the phase (clavicular portion, 42.0%; sternocostal portion, 42.3%).

Acceleration duration did not change reliably across the shooting series (adjusted end-to-start change −2.58 ms, 95% CI −11.08 to +6.51; q=0.589). Cocking duration showed a larger negative point estimate (−29.95 ms, 95% CI −73.29 to +1.86), but this change also did not meet the FDR criterion (q=0.153).

Neither phase duration was associated with ball velocity. Each additional 10 ms of acceleration was associated with +0.11 $km \cdot h^{-1}$ (95% CI −0.56 to +0.73; q=0.729), whereas each additional 10 ms of cocking was associated with −0.08 $km \cdot h^{-1}$ (95% CI −0.27 to +0.10; q=0.595). Thus, preserved ball velocity was not explained by a systematic change in cocking or acceleration duration. The corresponding performance-model estimates are summarized in Table 3.

3.7. Phase-specific changes across the shooting series

First-five to last-five changes in normalized RMS amplitude were heterogeneous across muscles and phases rather than uniformly increasing or decreasing (Figure 3B). Descriptively, the largest late-series increases were observed during deceleration for latissimus dorsi (+26.4 pp), pectoralis major, sternocostal portion (+15.4 pp), teres major (+11.7 pp), and lateral triceps (+8.9 pp), whereas thoracic erector spinae increased during acceleration (+12.1 pp).

In contrast, acceleration-phase amplitude decreased for flexor carpi radialis (−4.9 pp), middle deltoid (−4.4 pp), biceps brachii (−3.8 pp), middle trapezius (−3.6 pp), and anterior deltoid (−3.6 pp). Because amplitudes were normalized using athlete- and muscle-specific P95 references, these changes describe within-muscle variation across the series and should not be interpreted as absolute differences between muscles.

Changes in activation-weighted temporal centroid were smaller and likewise showed no common direction (Figure 3D). The largest later shifts were observed for flexor carpi radialis during deceleration (+5.0% of phase) and pectoralis major, clavicular portion during acceleration (+3.6%), whereas biceps brachii shifted earlier during cocking (−3.4%).

Overall, the first-five to last-five comparisons showed distributed phase-specific changes in activation amplitude and timing without a consistent montage-wide pattern. Figure 5B provides a focused visualization of the first-five and last-five phase-specific activation profiles of the two FDR-identified muscles.

Table 3: Integrated activation-fatigue-performance and phase-duration models.

Outcome	Estimate	95% CI	FDR q	Interpretation
All-muscle fatigue burden → velocity	+0.26 $km \cdot h^{-1}$ per SD	−0.59 to +1.15	0.846	No independent association
Amplitude-pattern distance → velocity, all-muscle model	+0.59 $km \cdot h^{-1}$	−0.73 to +1.84	0.846	No independent association
Temporal-pattern distance → velocity, all-muscle model	+0.03 $km \cdot h^{-1}$	−1.11 to +1.00	0.944	No independent association
All-muscle fatigue × amplitude-pattern distance	−0.32 $km \cdot h^{-1}$	−1.58 to +0.66	0.846	No interaction

Table 3: Integrated activation-fatigue-performance and phase-duration models.

Outcome	Estimate	95% CI	FDR q	Interpretation
All-muscle fatigue × temporal-pattern distance	+0.13 km·h^{-1}	−1.17 to +1.28	0.944	No interaction
Localized fatigue burden → velocity	−0.01 km·h^{-1} per SD	−0.67 to +0.59	0.997	No independent association
Amplitude-pattern distance → velocity, localized model	+0.41 km·h^{-1}	−0.89 to +1.76	0.817	No independent association
Temporal-pattern distance → velocity, localized model	−0.004 km·h^{-1}	−0.92 to +0.89	0.997	No independent association
Localized fatigue × amplitude-pattern distance	+0.50 km·h^{-1}	−0.94 to +1.64	0.761	No interaction
Localized fatigue × temporal-pattern distance	−1.07 km·h^{-1}	−2.46 to +0.28	0.277	No interaction
Acceleration duration → velocity	+0.11 km·h^{-1} per 10 ms	−0.56 to +0.73	0.729	No reliable association
Cocking duration → velocity	−0.08 km·h^{-1} per 10 ms	−0.27 to +0.10	0.595	No reliable association

3.8. Robustness analyses

The primary spectral findings were robust across alternative analytical specifications. Across the complete-montage sensitivity framework, all amplitude-adjusted standardized end-to-start contrasts remained negative and FDR-significant when continuous-wavelet and Fourier estimators, lower-frequency cutoffs of 20, 30, and 40 Hz, active-window restriction, and low-band trimming were applied (all $q \leq 0.0012$; Supplementary Table S5).

At the muscle-specific level, the two muscles identified in the primary analysis remained affected under the conservative ≥40-Hz analysis with concurrent amplitude adjustment: pectoralis major, clavicular portion showed an adjusted change of −5.69 Hz ($q=0.0008$), and teres major showed −12.79 Hz ($q=0.0165$).

Leave-one-athlete-out analyses yielded negative end-to-start estimates in every repetition for the complete-montage standardized contrast and for both FDR-identified muscles, indicating that the direction of the primary spectral findings was not driven by any single athlete.

The chronological permutation analysis was directionally consistent with the primary findings but did not independently meet the FDR criterion ($q=0.080$). It was therefore considered a secondary robustness check rather than independent statistical confirmation.

4. Discussion

The present study examined the myoelectric response to repeated maximal shooting in 14 professional water polo players using a 14-muscle throwing-side and trunk sEMG montage synchronized with movement-phase identification and ball-velocity assessment. Fatigue-compatible spectral changes were evaluated within a standardized late-cocking window, while phase-specific activation amplitude, temporal organization, movement-phase duration, and multimuscle pattern reorganization were examined across the shooting sequence. The main findings were that ball velocity remained preserved, whereas significant reductions in median frequency emerged selectively in the clavicular portion of pectoralis major and teres major. Changes in activation amplitude and timing were heterogeneous across the recorded musculature, and neither complete-montage nor localized measures of EMG reorganization were systematically associated with ball velocity. Together, these findings indicate that

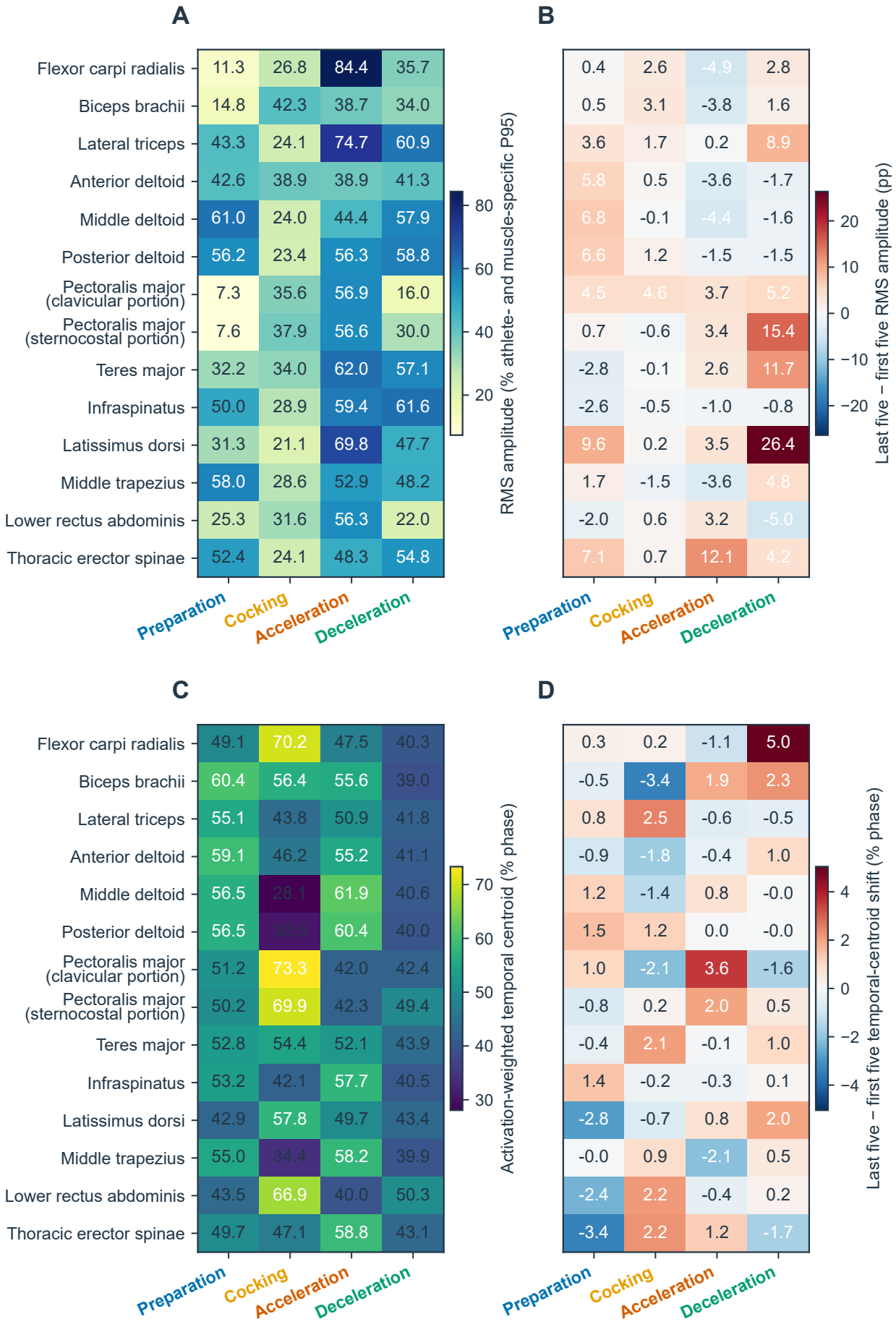


Figure 3: Phase-specific activation and temporal organization across the 14-muscle montage. (A) RMS amplitude. (B) First-five to last-five RMS-amplitude change. (C) Activation-weighted temporal centroid. (D) First-five to last-five temporal-centroid shift. pp, percentage points.

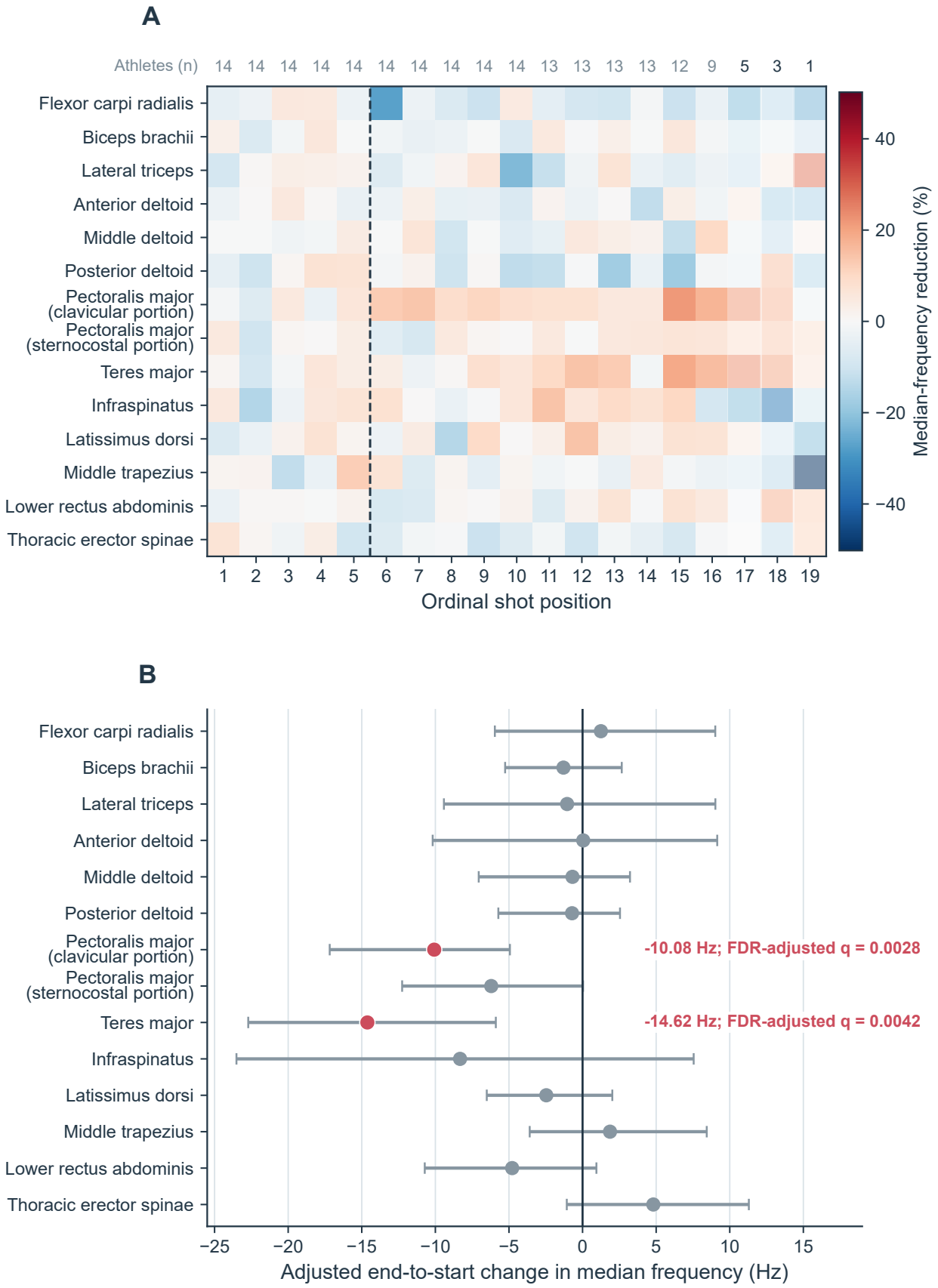


Figure 4: Fatigue-compatible spectral changes across the 14-muscle montage. (A) Shot-by-shot median-frequency reduction relative to the first-five reference. (B) Adjusted end-to-start change in median frequency; highlighted muscles survived FDR correction.

localized myoelectric alterations can develop during repeated maximal sport-specific actions without a concomitant deterioration in the primary external performance outcome.

The dissociation between preserved ball velocity and localized fatigue-compatible spectral change is one of the most relevant observations of the present study. Maintenance of the task outcome did not imply stability of the underlying myoelectric state. This interpretation is consistent with contemporary views of fatigability, according to which physiological adjustments may develop before they become evident as task failure or measurable performance loss [3]. A similar dissociation has previously been reported in water polo by Royal et al. [12], who found that increasing fatigue impaired aspects of shooting performance and technique while ball velocity remained comparatively resistant to deterioration. The present results extend this concept by showing that muscle-specific spectral alterations may also emerge despite preservation of ball speed. Importantly, the spectral effects identified here were not dependent on a single analytical specification: their direction was maintained across alternative lower-frequency cutoffs, wavelet and Fourier estimators, concurrent amplitude adjustment, active-window restriction, and leave-one-athlete-out analyses. The findings therefore support the possibility that, during a relatively short sequence of maximal sport-specific efforts, local myoelectric alterations may precede any detectable reduction in the primary performance variable.

The selective involvement of the clavicular portion of pectoralis major and teres major is biomechanically plausible, although the present data do not establish why these two muscles were preferentially affected. Both contribute to forceful shoulder actions relevant to overhead propulsion, including humeral adduction and internal rotation. Classic electromyographic investigations of throwing have identified pectoralis major among the muscles strongly activated during the propulsive phase, while skilled throwers appear to organize shoulder-muscle activity differently from less experienced performers [20]. More broadly, the throwing kinetic chain transfers motion and force generated by proximal segments through the shoulder and upper limb to the ball [21]. Experimental work on shoulder internal-rotation tasks has also demonstrated coordinated involvement of pectoralis major and teres major [22], and sport-dependent adaptations in shoulder-muscle activation during fatiguing internal-rotation exercise have been described in elite aquatic athletes, including water polo players [23]. In the present phase atlas, both the clavicular portion of pectoralis major and teres major showed acceleration-selective activation, further supporting the biomechanical plausibility of their involvement. However, the spectral outcome was measured during the final 200 ms of cocking, immediately before acceleration. The findings should therefore be interpreted as evidence that fatigue-compatible myoelectric alterations in these muscles were detectable before the propulsive phase, rather than as evidence that fatigue was generated specifically during acceleration.

Another important finding was that high relative activation did not necessarily correspond to greater fatigue-compatible spectral change. Flexor carpi radialis and lateral triceps showed some of the strongest acceleration-phase selectivity, yet neither demonstrated a reliable reduction in median frequency. Conversely, the two muscles showing significant spectral changes did not exhibit a uniform increase in RMS amplitude across the shooting sequence. This distinction is physiologically and methodologically important because amplitude- and frequency-domain sEMG measures provide complementary but non-equivalent information. Surface-EMG amplitude is influenced by motor-unit recruitment and discharge behavior, but also by action-potential cancellation, electrode–muscle geometry, muscle length, contraction velocity, and other factors that become particularly relevant during dynamic movements [4, 6, 7]. Spectral variables are likewise not direct readouts of a single physiological mechanism, because changes in muscle-fiber conduction, action-potential characteristics, motor-unit behavior, and recording geometry can all influence their values [24]. Accordingly, the present findings do not support a simple model in which repeated shooting produces fatigue that is accompanied by a uniform increase in RMS amplitude across the throwing musculature. Rather, the amplitude and spectral domains captured different aspects of the evolving myoelectric response, reinforcing the value of examining both during dynamic sport-specific tasks [4, 9].

The integrated analyses did not identify a single, common reorganization of the recorded EMG pattern that accounted for preservation of ball velocity. Neither the non-selected all-muscle fatigue burden nor amplitude-pattern or temporal-pattern distance was independently associated with ball velocity, and the corresponding interaction terms were also null. The secondary localized model led to the same

conclusion. These findings should not be interpreted as evidence that compensatory adjustments did not occur. Surface EMG captures only part of the neuromuscular coordination underlying a complex whole-body task, and inferring neural control strategies from changes in multimuscle surface signals requires caution [25]. Moreover, fatigue-related adaptation does not necessarily require wholesale reorganization of muscle coordination. Turpin et al. [26], for example, showed during cyclic exercise that fatigue-related adaptations could occur largely through changes in activation level while broader coordination patterns remained comparatively stable. In water polo, the range of possible mechanical solutions may be even greater because ball velocity depends on body elevation, trunk rotation, scapular control, upper-limb sequencing, and lower-limb support [10, 11, 21]. The heterogeneous first-to-last changes observed across muscles and phases, together with the absence of a montage-wide statistical pattern, are therefore more consistent with variable or athlete-specific adjustments than with a single universal compensation strategy. This interpretation is also compatible with previous evidence of substantial intraindividual movement variability during the 5-m water polo shot despite comparatively stable performance outcomes [15].

The temporal findings further argue against a simple mechanical explanation for preserved ball speed. Neither acceleration nor cocking duration changed reliably across the shooting series, and neither duration was associated with velocity. Players therefore did not appear to preserve performance by systematically extending the acceleration phase or by producing a consistent change in gross cocking duration. Activation-weighted temporal-centroid changes were likewise heterogeneous and generally small, with no common shift across the muscle montage. Ball velocity itself showed an initial rise followed by later attenuation rather than a progressive monotonic decline. Several mechanisms could theoretically contribute to such a trajectory, including familiarization, task-specific potentiation, progressive optimization of the shooting action, or competing effects of potentiation and accumulating fatigue. These mechanisms were not directly measured, however, and cannot be distinguished from the present dataset. The appropriate interpretation is therefore more limited: despite repeated maximal efforts and localized fatigue-compatible spectral changes, neither gross phase duration nor a common temporal reorganization of recorded muscle activity explained preservation of ball velocity.

Taken together, the present findings suggest short-term performance resilience during repeated maximal shooting in professional water polo players. The observable task outcome remained stable despite localized alterations in the myoelectric signal, indicating that preserved ball velocity should not be equated with absence of neuromuscular change. At the same time, the results should not be interpreted as evidence that the athletes were globally unfatigued or that the clavicular portion of pectoralis major and teres major alone determined the physiological cost of the task. The complete 14-muscle analysis instead showed that fatigue-compatible spectral manifestations were selective within the recorded montage, whereas activation amplitude and temporal organization changed heterogeneously across muscles and phases. The study therefore supports a distinction between external performance and local myoelectric state during repeated explosive sport actions. This interpretation remains physiological rather than causal: the present design demonstrates concurrent evolution of myoelectric characteristics and performance, but it cannot determine the specific mechanisms by which ball velocity was maintained.

4.1. Practical applications

From an applied perspective, ball velocity alone may underestimate the neuromuscular cost of repeated maximal shooting. In the present professional cohort, velocity remained preserved while two shoulder muscles already showed robust fatigue-compatible spectral changes. This finding does not imply that multichannel sEMG should routinely be used during training, but it suggests that stable ball speed should not automatically be interpreted as evidence of an unchanged muscular state. Shot volume, inter-shot recovery, technical quality, perceived exertion, body elevation, and shoulder symptoms may therefore provide useful complementary information when repeated maximal-shooting sets are prescribed.

The selective involvement of the clavicular portion of pectoralis major and teres major may also be relevant when considering conditioning and recovery strategies for repeated overhead shooting. However, these findings should not be translated into isolated strengthening or injury-prevention prescriptions. Water polo shooting depends on an integrated kinetic chain [21], and previous work in aquatic athletes indicates that fatigue-related shoulder activation patterns can differ according to sport-specific adaptation [23].

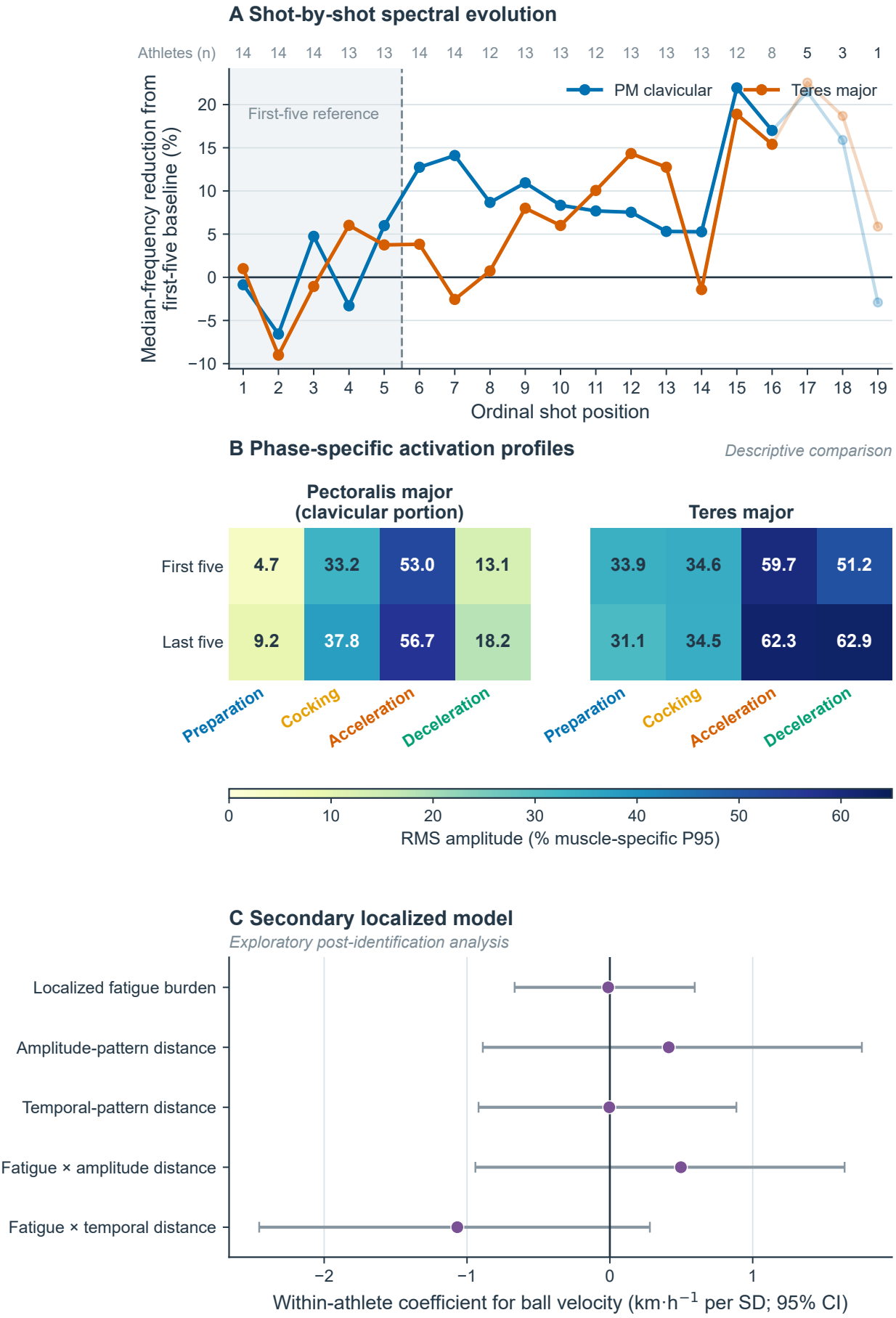


Figure 5: Localized myoelectric change and performance integration. (A) Shot-by-shot spectral evolution of the two FDR-identified muscles. (B) Descriptive first-five versus last-five phase-specific activation profiles. (C) Exploratory post-identification localized performance model.

The present results therefore support individualized monitoring of repeated-shooting load and recovery rather than a universal intervention focused on two muscles.

4.2. Strengths and limitations

Several features strengthen the present study. First, the protocol examined professional athletes performing a sport-specific maximal action rather than an isolated laboratory contraction. High-sampling-rate sEMG was synchronized with multi-view video and stereo-derived ball velocity, allowing local myoelectric behavior to be examined together with the external performance outcome. Second, the same 14-muscle montage was evaluated using explicit signal-quality criteria, and the primary spectral analysis was applied consistently across all recorded muscles. Third, the models accounted for concurrent RMS amplitude and within-athlete ball velocity, controlled multiplicity across the complete muscle set, and quantified uncertainty at the athlete level rather than treating repeated shots as statistically independent observations. The primary findings were also challenged through multiple alternative spectral specifications and leave-one-athlete-out analyses. Finally, separating the non-selected all-muscle burden from the post-identification localized burden reduced the risk of presenting the latter as independent confirmation of the two muscle-specific findings.

Several limitations nevertheless constrain interpretation. First, the study included only 14 male professional players from a single team. Although the repeated-shot design generated a relatively large number of observations, the number of independent athletes remained small, particularly for interaction analyses. The results therefore cannot automatically be generalized to female athletes, younger players, lower competitive levels, or athletes from other teams and training backgrounds. Second, surface EMG recorded during a rapid aquatic overhead movement is particularly vulnerable to changes in electrode–muscle geometry, motion artifact, amplitude cancellation, and cross-talk [6, 7, 25]. This is especially relevant when interpreting individual shoulder muscles, including teres major, and reinforces the need to describe the observed spectral changes as fatigue-compatible myoelectric manifestations rather than direct measures of local biochemical fatigue. Third, the study did not include direct measures of central or peripheral fatigue, muscle-fiber conduction velocity, metabolic state, perceived exertion, or local muscle oxygenation. The physiological mechanisms underlying the observed spectral changes therefore cannot be determined from the present dataset. Fourth, P95 amplitude normalization was specific to each athlete and muscle and consequently supports within-muscle comparisons across the shooting sequence but does not permit interpretation of absolute activation magnitude between different muscles. Finally, the shooting sequence represented a relatively brief repeated-effort protocol with approximately 5 s between shots. The findings should therefore be interpreted as characterizing short-term responses to repeated maximal shooting rather than the neuromuscular consequences of an entire match or prolonged training session.

5. Conclusion

Repeated maximal shooting in professional water polo produced selective fatigue-compatible myoelectric changes without a concomitant decline in ball velocity. Median-frequency reductions were confined to pectoralis major, clavicular portion, and teres major, whereas amplitude and temporal reorganization remained heterogeneous across the broader muscle montage. These findings indicate that preserved external performance can coexist with localized myoelectric alterations and support the use of muscle-specific sEMG measures alongside performance outcomes when evaluating fatigue during repeated maximal shooting.

Declarations

Declaration	Statement
Author Contributions	Conceptualization, N.L.B., F.C. and L.P.; Methodology, F.C., H.İ.C. and L.P.; Formal analysis, N.L.B., F.C. and H.İ.C.; Investigation, F.C. and L.P.; Data curation, F.C. and H.İ.C.; Writing – original draft, F.C.; Writing – review & editing, H.İ.C. and L.P.; Visualization, F.C. and H.İ.C.; Supervision, L.P.; Project administration, L.P. All authors have read and agreed to the published version of the manuscript.
Funding	This research received no external funding.
Institutional Review Board Statement	The study was conducted in accordance with the Declaration of Helsinki and was approved by the Comitato Etico per la Ricerca di Ateneo (CERA; approval no. 2024.55, 14 June 2024).
Informed Consent Statement	Written informed consent was obtained from all participants involved in the study.
Data and Code Availability	The de-identified processed datasets, complete analysis tables, and analysis code supporting the findings of this study are available from the corresponding author upon reasonable request.
Acknowledgments	The authors have no acknowledgments to report.
Competing Interests	The authors declare no commercial, financial, or other relationships that could be construed as a potential conflict of interest.
Supplementary Materials	Supplementary Tables S1–S5 and Supplementary Figure S1. Table S1: Data quality; Table S2: FDR-significant amplitude phase-selectivity contrasts; Table S3: Complete-montage muscle-specific spectral models; Table S4: Integrated all-muscle and localized fatigue models; Table S5: Complete-montage spectral sensitivity analyses; Figure S1: Observed peak-phase amplitude contrasts across the 14-muscle montage.
Generative AI Disclosure	No type of AI was used

[1] Gandevia SC. Spinal and supraspinal factors in human muscle fatigue. Physiological Reviews. 2001;81(4):1725–89. https://doi.org/10.1152/physrev.2001.81.4.1725

[2] Allen DG, Lamb GD, Westerblad H. Skeletal muscle fatigue: Cellular mechanisms. Physiological Reviews. 2008;88(1):287–332. https://doi.org/10.1152/physrev.00015.2007

[3] Enoka RM, Duchateau J. Translating fatigue to human performance. Medicine & Science in Sports & Exercise. 2016;48(11):2228–38. https://doi.org/10.1249/MSS.0000000000000929

[4] Cifrek M, Medved V, Tonković S, Ostojić S. Surface EMG based muscle fatigue evaluation in biomechanics. Clinical Biomechanics. 2009;24(4):327–40. https://doi.org/10.1016/j.clinbiomech.2009.01.010

[5] González-Izal M, Malanda A, Gorostiaga EM, Izquierdo M. Electromyographic models to assess muscle fatigue. Journal of Electromyography and Kinesiology. 2012;22(4):501–12. https://doi.org/10.1016/j.jelekin.2012.02.019

[6] Merletti R, Cerone GL. Tutorial. Surface EMG detection, conditioning and pre-processing: Best practices. Journal of Electromyography and Kinesiology. 2020;54:102440. https://doi.org/10.1016/j.jelekin.2020.102440

[7] Farina D. Interpretation of the surface electromyogram in dynamic contractions. Exercise and Sport Sciences Reviews. 2006;34(3):121–7. https://doi.org/10.1249/00003677-200607000-00006

[8] Merlo E, Pozzo M, Antonutto G, Prampero PE di, Merletti R, Farina D. Time-frequency analysis and estimation of muscle fiber conduction velocity from surface EMG signals during explosive dynamic contractions. Journal of Neuroscience Methods. 2005;142(2):267–74. https://doi.org/10.1016/j.jneumeth.2004.09.002

[9] Puce L, Pallecchi I, Marinelli L, Mori L, Bove M, Diotti D, Ruggeri P, Faelli E, Cotellessa F, Trompetto C. Surface electromyography spectral parameters for the study of muscle fatigue in swimming. Frontiers in Sports and Active Living. 2021;3:644765. https://doi.org/10.3389/fspor.2021.644765

[10] Elliott BC, Armour J. The penalty throw in water polo: A cinematographic analysis. Journal of Sports Sciences. 1988;6(2):103–14. https://doi.org/10.1080/02640418808729801

[11] McCluskey L, Lynskey S, Leung CK, Woodhouse D, Briffa K, Hopper D. Throwing velocity and jump height in female water polo players: Performance predictors. Journal of Science and Medicine in Sport. 2010;13(2):236–40. https://doi.org/10.1016/j.jsams.2009.02.008

[12] Royal KA, Farrow D, Mujika I, Halson SL, Pyne D, Abernethy B. The effects of fatigue on decision making and shooting skill performance in water polo players. Journal of Sports Sciences. 2006;24(8):807–15. https://doi.org/10.1080/02640410500188928

[13] Yaghoubi M, Moghadam A, Khalilzadeh MA, Shultz SP. Electromyographic analysis of the upper extremity in water polo players during water polo shots. International Biomechanics. 2014;1(1):15–20. https://doi.org/10.1080/23335432.2014.976591

[14] Yaghoubi M, Esfehani MM, Hosseini HA, Alikhajeh Y, Shultz SP. Comparative electromyography analysis of the upper extremity between inexperienced and elite water polo players during an overhead shot. Journal of Applied Biomechanics. 2015;31(2):79–87. https://doi.org/10.1123/jab.2014-0068

[15] Taylor PG, Landeo R, Coogan J. Intraindividual movement variability within the 5 m water polo shot. Journal of Applied Biomechanics. 2014;30(3):477–82. https://doi.org/10.1123/jab.2013-0133

[16] Hermens HJ, Freriks B, Disselhorst-Klug C, Rau G. Development of recommendations for SEMG sensors and sensor placement procedures. Journal of Electromyography and Kinesiology. 2000;10(5):361–74. https://doi.org/10.1016/S1050-6411(00)00027-4

[17] Besomi M, Devecchi V, Falla D, et al. Consensus for experimental design in electromyography (CEDE) project: Checklist for reporting and critically appraising studies using EMG (CEDE-check). Journal of Electromyography and Kinesiology. 2024;76:102874. https://doi.org/10.1016/j.jelekin.2024.102874

[18] Besomi M, Hodges PW, Clancy EA, et al. Consensus for experimental design in electromyography (CEDE) project: Amplitude normalization matrix. Journal of Electromyography and Kinesiology. 2020;53:102438. https://doi.org/10.1016/j.jelekin.2020.102438

[19] Benjamini Y, Hochberg Y. Controlling the false discovery rate: A practical and powerful approach to multiple testing. Journal of the Royal Statistical Society: Series B. 1995;57(1):289–300. https://doi.org/10.1111/j.2517-6161.1995.tb02031.x

[20] Gowan ID, Jobe FW, Tibone JE, Perry J, Moynes DR. A comparative electromyographic analysis of the shoulder during pitching. Professional versus amateur pitchers. American Journal of Sports Medicine. 1987;15(6):586–90. https://doi.org/10.1177/036354658701500611

[21] Chu SK, Jayabalan P, Kibler WB, Press J. The kinetic chain revisited: New concepts on throwing mechanics and injury. PM&R. 2016;8(3 Suppl):S69–77. https://doi.org/10.1016/j.pmrj.2015.11.015

[22] Alizadehkhaiyat O, Hawkes DH, Kemp GJ, Frostick SP. Electromyographic analysis of shoulder girdle muscles during common internal rotation exercises. International Journal of Sports Physical Therapy. 2015;10(5):645–54.

[23] King S, Dong L, Caron M, Côté JN. Changes in muscle activation during and after a shoulder-fatiguing task: A comparison of elite female swimmers and water polo players. Frontiers in Sports and Active Living. 2022;4:881582. https://doi.org/10.3389/fspor.2022.881582

[24] Dimitrova NA, Dimitrov GV. Interpretation of EMG changes with fatigue: Facts, pitfalls, and fallacies. Journal of Electromyography and Kinesiology. 2003;13(1):13–36. https://doi.org/10.1016/S1050-6411(02)00083-4

[25] Hug F. Can muscle coordination be precisely studied by surface electromyography? Journal of Electromyography and Kinesiology. 2011;21(1):1–12. https://doi.org/10.1016/j.jelekin.2010.08.009

[26] Turpin NA, Guével A, Durand S, Hug F. Fatigue-related adaptations in muscle coordination during a cyclic exercise in humans. Journal of Experimental Biology. 2011;214(19):3305–14. https://doi.org/10.1242/jeb.057133